ELSEVIER

Materials Science and Engineering B 127 (2006) 22–28

MATERIALS SCIENCE & ENGINEERING B

www.elsevier.com/locate/mseb

Investigation of chromium carbide/alumina nano-composite prepared via MOCVD in fluidized bed and densification process

Hao-Tung Lin [a], Wei-Sheng Huang [a], Sheng-Chang Wang [b], Horng-Hwa Lu [c], Wen-Cheng J. Wei [d], Jow-Lay Huang [a,*]

[a] *Department of Materials Science and Engineering, National Cheng Kung University, No. 1, Ta-Hsueh Road, Tainan 701, Taiwan, ROC*
[b] *Department of Mechanical Engineering, Southern Taiwan University of Technology, Tainan 710, Taiwan, ROC*
[c] *Department of Mechanical Engineering, National Chin-Yi Institute of Technology, Taichung 411, Taiwan, ROC*
[d] *Department of Materials Science and Engineering, National Taiwan University, Taipei 106, Taiwan, ROC*

Received 9 June 2005; received in revised form 8 August 2005; accepted 8 September 2005

Abstract

Nano-sized Cr-species particles with a size about 20–40 nm, uniformly coated on alumina particles, has been prepared by metal organic chemical vapor deposition (MOCVD) in the fluidized chamber, using the pyrolysis of $Cr(CO)_6$ precursor. The Carbothermal reactions of Cr-species in an Ar atmosphere in a graphite furnace at 1250 °C for 2 h and the microstructure of high pressure sintering specimen are reported. The crystalline phase of the powder deposited in fluidized bed was characterized by an X-ray diffractometer, and transmission electron microscopy. The analysis indicates that the deposited powders were metastable CrC_{1-x} and Cr_2O_3. These Cr-species were transferred into stable chromium carbide (Cr_3C_2 and Cr_7C_3) after the thermal treatment as well as high pressure sintering. Microstructure of sintering specimen shows that the cluster of coating nano-particles were formed in the fluidized bed which coarsen during densification and generally located on the grain boundary to inhibit the alumina grain growth. Further, the independent coating nano-particle was also incorporated into the alumina grains.

Keywords: MOCVD; Alumina; Nano-particle

1. Introduction

Alumina (Al_2O_3) is one of the most widely used ceramic materials because of its excellent physical, thermal and chemical properties, but its intrinsic brittleness and relatively poor reliability make the toughening of alumina ceramics an important and challenging area. Among the reported toughening methods [1–4], the incorporation of hard particulate reinforcement has been proven to be an easy, safe and economical toughening technique for alumina ceramics. Chromium carbide has been successfully incorporated into Al_2O_3 [1] for toughening purposes owing to its high Young's modulus and its high temperature erosion resistance. Quite promising mechanical properties and high temperature oxidation resistance of chromium carbide/alumina composites have been previously reported in the literature [1,5–7]. The advantages of the addition of ultrafine inclusions have been reported by Nakahira and Niihara [8]. These are the reduction in grain size of the matrix grains, and the strengthening and toughening of the composites. Various methods such as gas condensation [9], laser induced pyrolysis [10], sol–gel [11,12], microwave plasma [13] and gamma radiation [14] synthesis have been investigated for synthesizing nano-size particles. Furthermore, using traditional mixing techniques for preparing particle-reinforced composite, the nano-scaled reinforced particles are difficult to disperse uniformly on the micro-scale matrix particles. This problem is ascribed to the fact that nano-scale particles agglomerate easily due to the interaction between the particles. It was recognized [15] that a fluidized bed reactor can supply an environment with a uniform temperature and concentration of the coating precursor, which can provide the possibility of a good dispersion of reinforcing nano-particles in a matrix. A precursor vaporized at a low temperature is the major characteristic of the metal–organic chemical vapor deposition (MOCVD) process. The combination of conventional fluidized bed technology with standard chemical vapor deposition has been proven to be an effective method to

* Corresponding author. Tel.: +886 6 234 8188; fax: +886 6 276 3586.
E-mail address: JLH888@mail.ncku.edu.tw (J.-L. Huang).

0921-5107/$ – see front matter © 2005 Elsevier B.V. All rights reserved.
doi:10.1016/j.mseb.2005.09.006

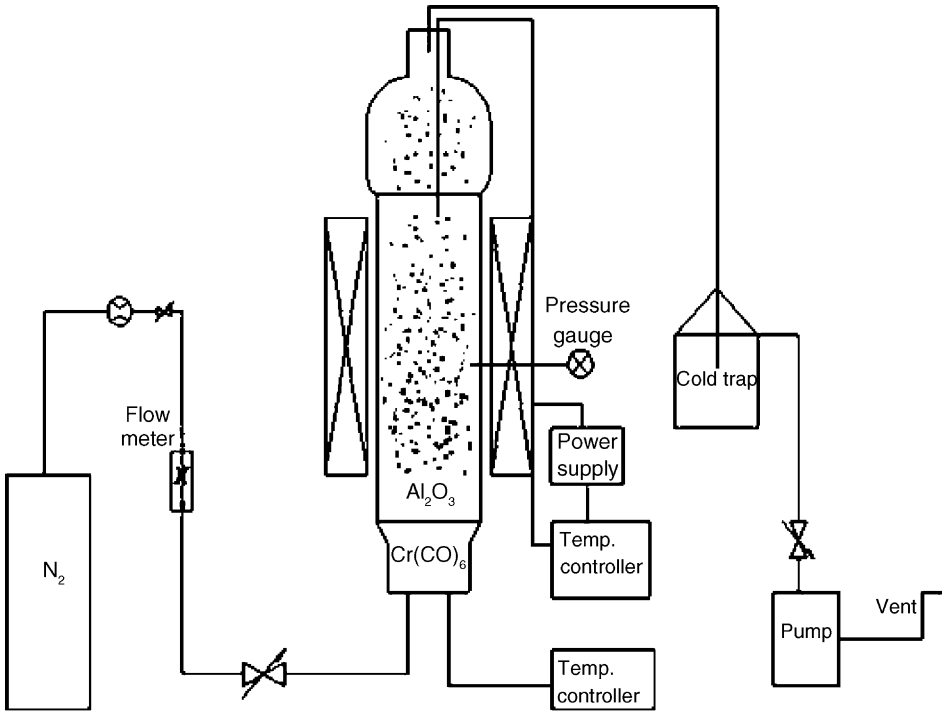

Fig. 1. Schematic diagram of MOCVD in fluidized bed reactor.

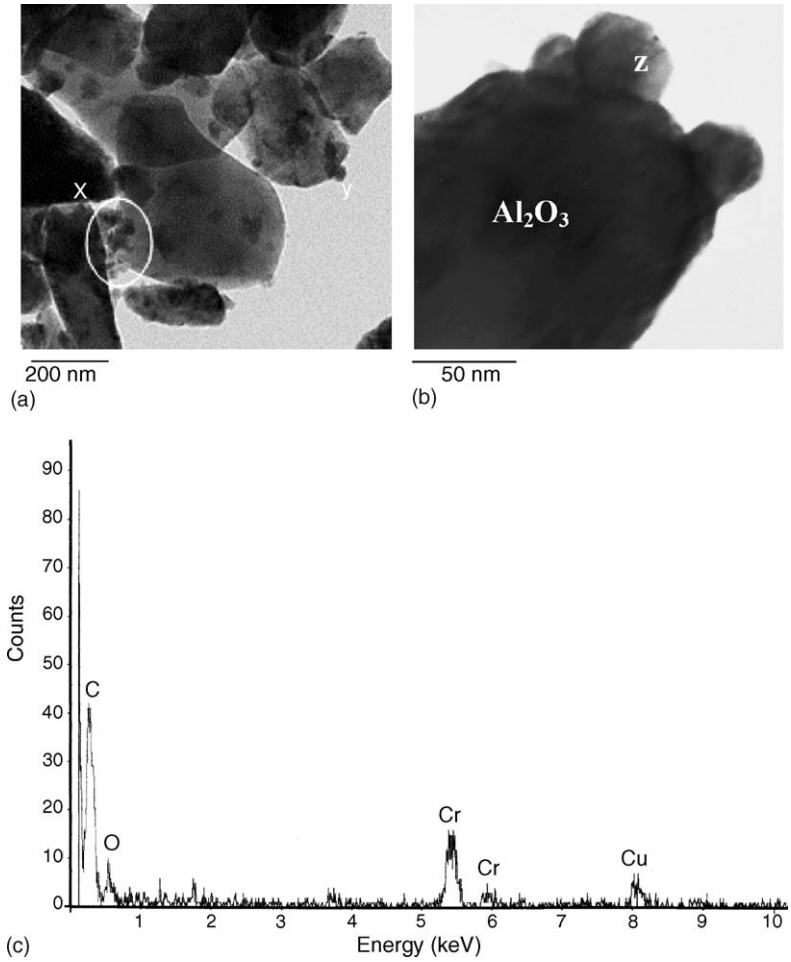

Fig. 2. (a and b) TEM micrographs of as-deposited particle prepared by MOCVD in fluidized bed at 400 °C in N_2, showing the nano-sized Cr-species particles coated on micro-sized Al_2O_3 particle. "x" is a cluster nano-particles, "y" is a single nano-particle (c) EDS spectrum of the coating particle "z" in (b).

deposit particles [16,17]. In this study, a fluidized powder reactor was used for MOCVD processes to produce the nano-sized particles coated on to Al_2O_3 particles with a micron grain size. The carbonizing of the nano-sized particles, the sintering behaviors and microstructure of the composites were also discussed in this study.

2. Experiment

Chromium hexacarbonyl ($Cr(CO)_6$, 99%, Strem Chemicals Co., USA) was used as a precursor for chromium oxide in the MOCVD process. Aluminum oxide powder (A16SG, Alcoa, USA) was used as the matrix powder. The vapor of the precursor was carried by N_2 gas (99.9% pure) that was introduced into the fluidized bed reactor for the MOCVD process.

Based on Lander's report [18], the precursor container was kept at 75 °C in a vacuum (10 Torr) in the present study. Hexacarbonyl vapor, which was carried by N_2 gas, was decomposed in the hot chamber (where the temperature was maintained at 400 °C) and then the decomposed species would deposit on the fluidizing alumina particles. A schematic diagram of the apparatus is shown in Fig. 1.

The as-deposited particles were characterized by X-ray diffractrometry (Rigaku D/MaxII, Japan). Field Emission Transmission Electron Microscopy (FETEM, Hitachi FE-2000, Japan) equipped with energy dispersive X-ray spectroscopy (EDS, England) was used to identify phase, morphology and composition. The as-deposited powder was ball-milled for 24 h and sieved through a 200-mesh screen. The sieved powder was then thermally treated at 1250 °C for 2 h in an Ar atmosphere in a graphite furnace. The ball-milled and screened powder, used as the sintering powder, was high pressed at 1400 °C under a mechanical pressure of 25 MPa for 1 h (High-multi-5000, Fujidempa Kogyo Co., LTD., Japan) under vacuum (10^{-3} Torr). The microstructure and phases of the sintered samples were also characterized by XRD, SEM (XL-40 FEG Field Emission Scanning Electron Microscope, Philip Co., Holland) and TEM. At least five samples were analyzed to acquire electron diffraction patterns and reliably identify the corresponding phases.

3. Results and discussion

3.1. The characteristics of as-deposited powders

TEM micrographs of the as-deposited powder prepared at 400 °C in the fluidized bed are shown in Fig. 2(a and b). Fig. 2(a) shows nano-particles disperses well on Al_2O_3 particles. Fig. 2(b) indicates that the nano-particles with about 20–40 nm were coated on Al_2O_3 particle. Fig. 2(c) is the EDS spectrum of the coating particle "z" shown in Fig. 2(b), which clearly reveals the composition of C, Cr and O elements. The Cu intensity coming from the Cu grid was also detected. The EDS results showed evidence that the coated particles resulted from pyrolysis coating by the Cr-precursor.

Fig. 3 shows the TEM diffraction pattern of nanometer-sized particles dispersed on the alumina surface of the particles as shown in Fig. 2(a). The TEM diffraction patterns, indicate that

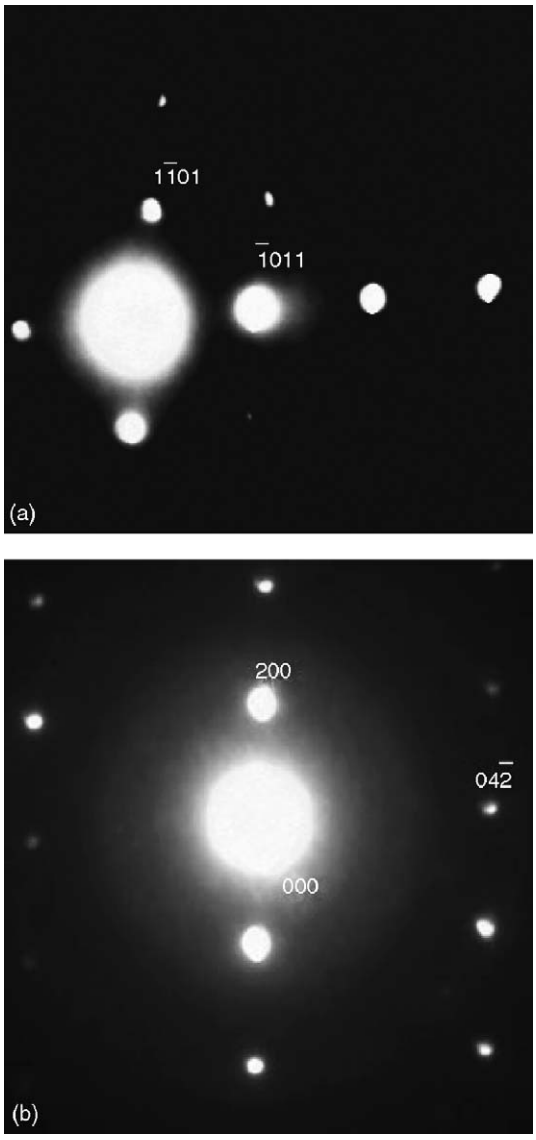

Fig. 3. TEM diffraction patterns of the coating particles of (a) Cr_2O_3 phase with hexagonal structure and (b) CrC_{1-x} phase with NaCl (B1) structure, respectively.

the coating particles were Cr_2O_3 with hexagonal crystalline structure and a CrC_{1-x} phase a with NaCl (B1) structure [19], as shown in Fig. 3(a and b), respectively. From our previous research [20], in addition to the chromium carbide (CrC_{1-x}), free carbon also existed in the as-deposited powder. These results are similar to the finding by Schuste and Maury [21]. They reported that the CrC_{1-x} phase was fabricated in the coating when $Cr(CO)_6$ was used as the precursor of a MOCVD process. Bouzy et al. [19] indicated that non-stoichiometric CrC_{1-x} is a metastable phase, and interpreted that small C atoms were inserted in the octahedral interstitial sites of the cubic-close Cr packings in this structure.

3.2. Carbothermal reaction of chromium-species

Fig. 4 shows the TEM morphology and diffraction patterns of the as-deposited powder treated at 1250 °C for 2 h in an Ar atmosphere in a graphite furnace. Compared to the as-deposited

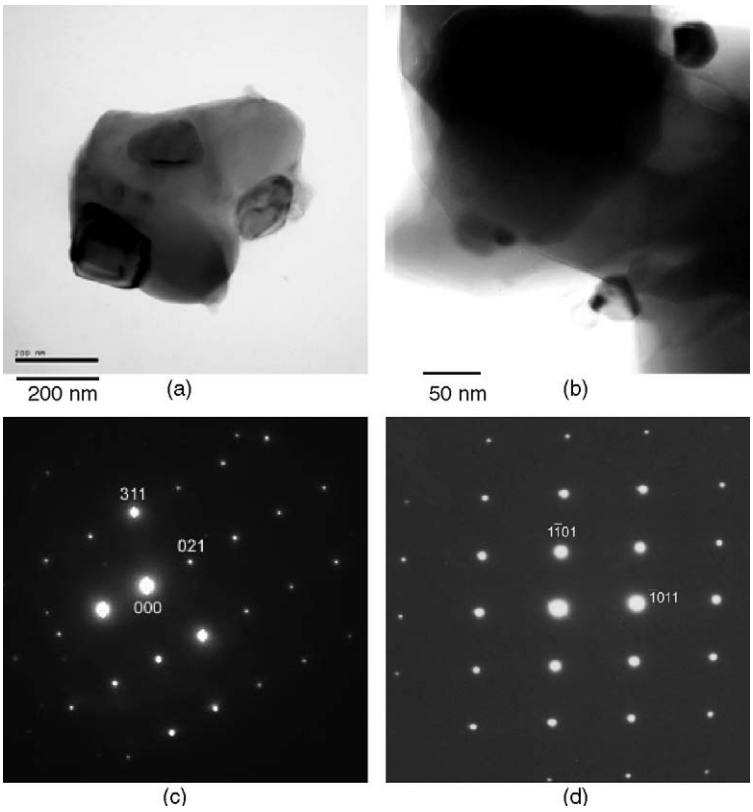

Fig. 4. (a and b) TEM micrographs of composite powder treated at 1250 °C in a graphite furnace under an argon atmosphere for 2 h, which the coating particles are about 100 and 30 nm in size, respectively. (c) TEM diffraction patterns of coating particles treated under above condition, showing a Cr_3C_2 phase with a orthorhombic structure and (d) showing a Cr_7C_3 phase with a hexagonal structure.

particles, the particle size shown in Fig. 4(a) increases from 20–40 to 80–100 nm. The growth was due to the coalescence of the cluster of nanometer-size particles as "x" in Fig. 2(a) during thermal treatment. Whereas the thermal treated particles shown in Fig. 4(b) keep the same size with the as-deposited, similar to the single coating particle like "y" in Fig. 2(a). Fig. 4(c and d) indicate the TEM diffraction patterns of coating particles, showing the Cr_3C_2 phase with an orthorhombic structure and the Cr_7C_3 phase with a hexagonal structure, respectively. Fig. 5 presents the XRD results for the powder heated under the thermal treatment, which is consistent with the observation made in the TEM diffraction patterns. It can thus be concluded that Cr_7C_3 and Cr_3C_2 form on the surface of the alumina after the heat treatment. In the case of the metastable CrC_{1-x} phase, according to the results of Bewilogua et al. [22], an annealing treatment would cause the transformation of the CrC_{1-x} into the stable Cr_3C_2. In this study, the CrC_{1-x} reacts with free carbon and can transform to Cr_3C_2. The carbonization of Cr_2O_3 has been previously explained [23–25]. Equations of the carbothermal reaction processes of Cr_2O_3 can be shown as following reactions [26]:

$$Cr_2O_3 + \frac{13}{3}C \rightarrow \frac{2}{3}Cr_3C_2 + 3CO,$$
$$\Delta G = 754746.567 - 543.87T \quad (1)$$

$$Cr_2O_3 + \frac{27}{7}C \rightarrow \frac{2}{7}Cr_7C_3 + 3CO,$$
$$\Delta G = 757079.56 - 543.86T \quad (2)$$

Hernandez et al. [23] reported that the graphite mould introduced carbon radicals into the Cr_2O_3 powders, and promoted it conversion to Cr_7C_3 during thermal treatment to be carried out

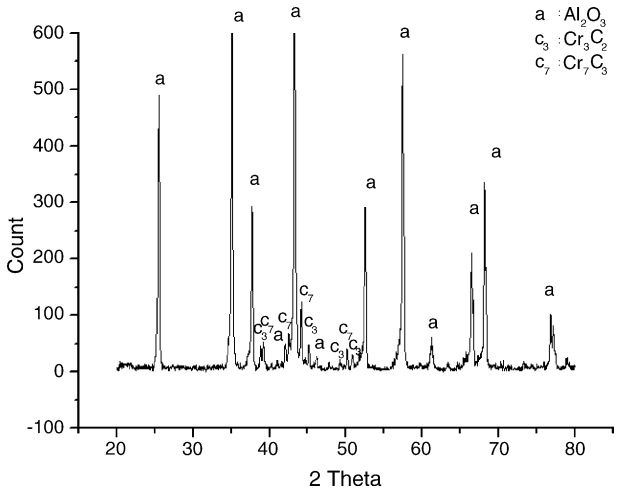

Fig. 5. XRD patterns of as-deposited powder at 1250 °C for 2 h in an Ar atmosphere in a graphite furnace.

Table 1
Carbon content of specimen

Fabricated in fluidized reactor	400 °C, 2 h
Carbon content (%)	0.23

in a graphite furnace. Chu and Rahmel [24] also suggested the carbonizing behaviors to be relevant to the activity of carbon. In their report, a piece of graphite felt was placed directly in front of the Cr_2O_3 tablet during thermal treatment and led to a greater formation of Cr_3C_2 surface particles, owing to the higher carbon activity in this system. Otherwise, the Cr_7C_3 phase would be generated during the carbonizing process. Antony et al. [25] also reported that the Cr_3C_2 phase was initially generated from the interface region between Cr_2O_3 and C. In this study, the existence of a Cr_7C_3 phase was due to not all of the Cr_2O_3 particles in the fluidizing powder were directly in contact with the free carbon. Therefore, it is reasonable for the Cr_3C_2 and Cr_7C_3 phases to form simultaneously from the Cr_2O_3 particles during the thermal treatment (Table 1).

3.3. Microstructure development of sintered samples

The powder fabricated by the fluidized bed process at 400 °C after the ball-milling and screening was used for hot-pressed sintering. Fig. 6 shows the XRD patterns of chromium carbide/alumina composite prepared by hot-pressing at 1400 °C in a vacuum for 1 h. The peaks indicate the carbide phase was a mixture of phases of Cr_7C_3 and Cr_3C_2. The TEM micrograph of sintered chromium carbide/alumina nano-composites is shown in Fig. 7. The ratio of atom percentage between Cr and Al is expressed in Eq. (3):

$$r = \frac{A_{Cr}}{A_{Al}} \tag{3}$$

The atomic ratios (r) of grains A–C in Fig. 7 are shown in Table 2, which indicates that Cr ions diffused into the Al_2O_3 matrix and the Cr_2O_3–Al_2O_3 solid solution produced. According to the report of Sternitzke [27], the nano-sized particle (P)

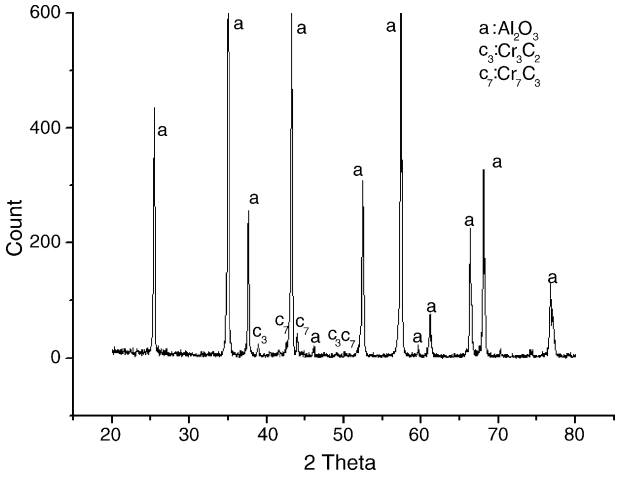

Fig. 6. XRD patterns of chromium carbide/alumina composite hot pressed at 1400 °C in a graphite furnace in a vacuum for 1 h.

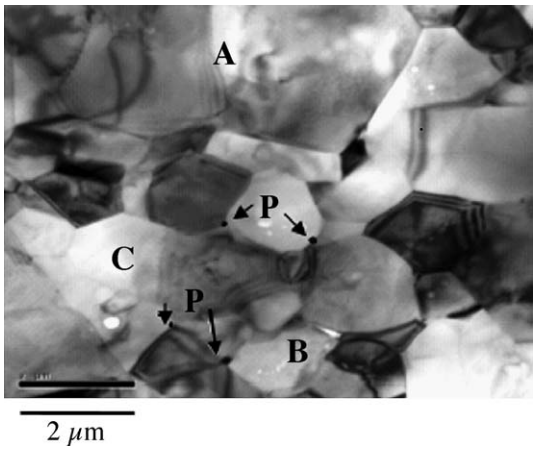

Fig. 7. Bright field image of TEM micrograph of chromium carbide/alumina nano-composite hot pressed at 1400 °C in a vacuum for 1 h.

shown in Fig. 7 pinned the matrix grain boundaries and inhibited the Al_2O_3 grain growth. Therefore, the Al_2O_3 grain nearby nano-sized particles as indicated in the figure, was smaller than others.

Fig. 8 shows the bright field image of TEM micrographs of sintered nano-composites. Fig. 8(a) shows the Cr-carbide particles marked "D" located on a triple junction. Fig. 8(b) is the higher magnification of Fig. 8(a). The dark field image is also shown in the right-upper corner of Fig. 8(b). It indicates that the particle "D" is composed of nano-particles d1 and d2. A similar condition was also observed in Fig. 8(c and d), which show that "E" was composed of e1, e2 and e3. The grain boundaries between the nano-particles were suspected to exist due to non-coalescence of grains in the final step of sintering. The non-consolidation of nano-particles was ascribed to the pore easily becoming a residue in triple-junction area, which retards the coalescence of nano-particles. The intergranular chromium carbide particle with micron-size marked "F", as shown in Fig. 8(e) tended to stay at the triple-junction and suppressed the grain growth of the matrix because of the pinning force exerted on the grain boundary. It is similar to the reports [28,29], which indicates that the reinforced second phase led to narrower distribution of alumina grain size. Fig. 8(f) shows intragranular nano-sized particles, indicated by "G", enclosed in an Al_2O_3 grain with a size of about 30 nm, which approximately equals the original size of as-deposited powder fabricated in a fluidized bed. This implies that the nano-particles stop coarsening when they were trapped in the Al_2O_3 grain during sintering.

From the above discussion, it was found that the Cr_2O_3 particle had at least two reactions during sintering. One was that the system Al_2O_3–Cr_2O_3 formed due to the continuous solid

Table 2
Ratio (r) of Cr to Al atom percentage on grains A–C (in Fig. 7)

Grain	$r = A_{Cr}/A_{Al}$
A	1.73×10^{-2}
B	1.12×10^{-2}
C	0.86×10^{-2}

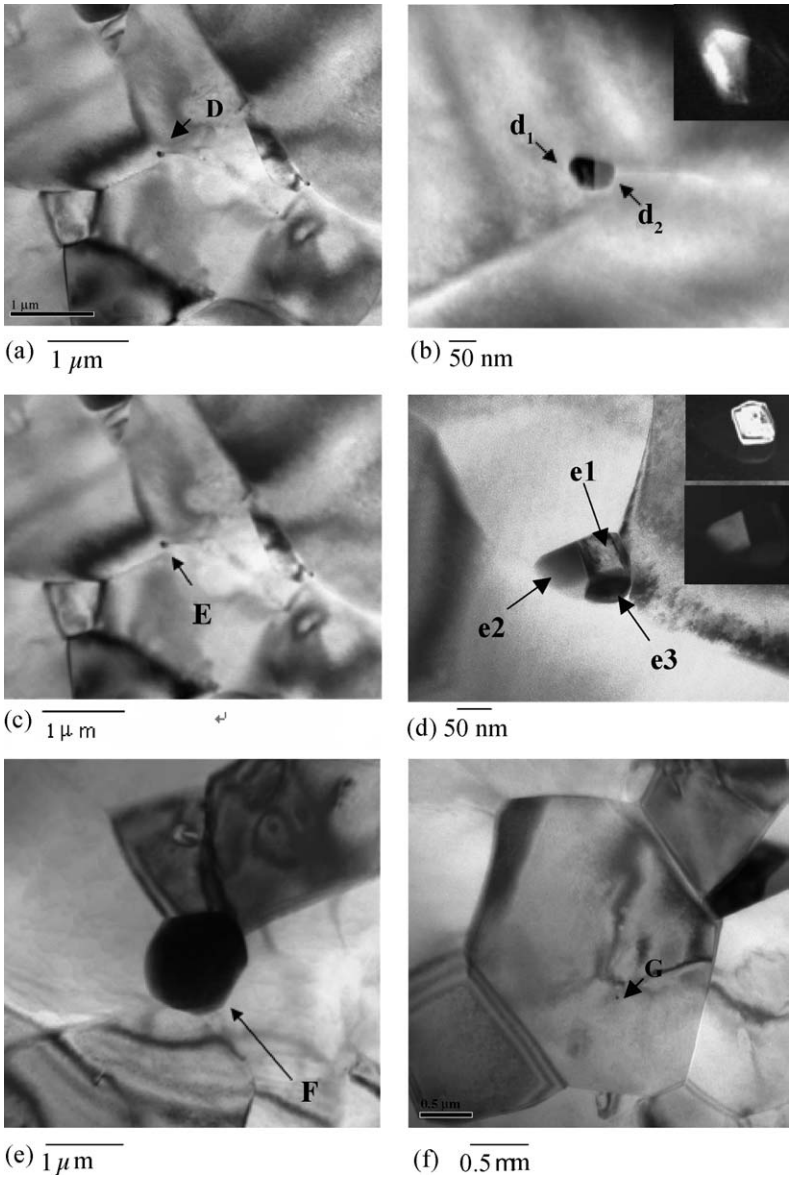

Fig. 8. Bright field image of TEM micrographs of intergranular (a) nano-sized particles "D" located on triple junction areas, (b) bright and dark-field micrographs in higher magnification of particle "D" in (a), (c) particles located on triple junction areas, (d) bright and dark-field micrographs in higher magnification of particle "E" in (c), (e) intergranular micron-sized particle "F" and (f) intragranular nano-sized particle "G".

solution in the system [30]. Another one was that Cr_2O_3 particles reacted with carbon or carbon radicals to induce Cr-carbide (Cr_3C_2 or Cr_7C_3).

4. Conclusions

A fluidized powder reactor used for MOCVD processes is an efficient method to prepare Cr-species nano-powder/ceramic composite powders. Nano-sized Cr-species particles were deposited uniformly on the surfaces of Al_2O_3 powders, which were ascribed to the characteristic of very large heat and mass transfer rates in the fluidized bed. The as-deposited powder with CrC_{1-x} and Cr_2O_3 was detected. The CrC_{1-x} transferred into a Cr_3C_2 phase during thermal treatment, while the Cr_2O_3 transferred to a mixture of Cr_3C_2 and Cr_7C_3. In case of Cr_2O_3 particles, there were two reactions that took place in the sintering process. One was the system Al_2O_3–Cr_2O_3 forming a solid solution, and the second one was the Cr_2O_3 particles reacting with carbon particles or carbon radicals to induce Cr-carbide. Intergranular and non-consolidation nano-sized Cr-carbide particles were observed at triple-junctions. In general, the coarse Cr-carbide particles tended to located on grain boundaries, which impeded the alumina grain growth whilst nano-partilces which were incorporated into the alumina grains due to sintering of the nano-particles were probably pass over by the grain boundary movement associated with the typical densification mechanism.

Acknowledgment

The authors would like to thank the National Science Council of the Republic of China for its financial support under the Contract No. NSC-92-2216-E-006-011.

References

[1] C.T. Fu, J.M. Wu, A.K. Li, J. Mater. Sci. 29 (1994) 2671–2677.
[2] S. Lio, M. Watanabe, M. Matsubara, Y. Matsuo, J. Am. Ceram. Soc. 72 (10) (1989) 1880–1884.
[3] W.J. Tseng, P.D. Funkenbusch, J. Am. Ceram. Soc. 75 (5) (1992) 1171–1175.
[4] Y.S. Chou, D.J. Green, J. Am. Ceram. Soc. 75 (12) (1992) 3346–3352.
[5] C.T. Fu, A.K. Li, J.M. Wu, J. Mater. Sci. 28 (1993) 6285–6294.
[6] K.M. Shu, C.T. Fu, D.M. Liu, J. Mater. Sci. Lett. 13 (1994) 1146–1148.
[7] C.T. Fu, A.K. Li, J.M. Wu, J.M. Wu, Br. Ceram. Trans. 93 (5) (1994) 178–182.
[8] A. Nakahira, K. Niihara, J. Ceram. Soc. Jpn. 100 (1992) 448–453.
[9] U. Balachandran, R.W. Siegel, Y.X. Liao, T.R. Askew, Nanostruct. Mater. 5 (1995) 505–512.
[10] G. Peters, K. Jerg, B. Schramm, Mater. Chem. Phys. 55 (1998) 197–201.
[11] M. Chatterjee, B. Siladitya, D. Ganguli, Mater. Lett. 25 (1995) 261–263.
[12] A. Kawabata, M. Yoshinaka, K. Horota, O. Yamaguchi, J. Am. Ceram. Soc. 78 (8) (1995) 2271–2273.
[13] D. Vollath, D.V. Szabó, J.O. Willis, Mater. Lett. 29 (1996) 271–279.
[14] Y. Zhu, Y. Qian, M. Zhang, Mater. Sci. Eng. B41 (1996) 294–296.
[15] D. Kunii, O. Levenspiel, Fluidization Engineering, Huntington, NY, 1977, pp. 195–223.
[16] B.J. Wood, A. Sanjurjo, G.T. Tong, S.E. Swider, Sur. Coat. Tech. 49 (1991) 228–232.
[17] K. Tsugeki, T. Kato, Y. Koyanagi, K. Kusakabe, S. Morooka, J. Mater. Sci. 28 (1993) 3168–3172.
[18] J.J. Lander, L.H. Germer, Am. Inst. Min. Metall. Tech. 14 (6) (1947) 1–42.
[19] E. Bouzy, E. Bauer-Grosse, G. Le Caer, Philos. Mag., B. 68 (5) (1993) 619–638.
[20] H.T. Lin, J.L. Huang, W.T. Lo, W.C.J. Wei, J. Mater. Res. 20 (8) (2005) 2154–2160.
[21] F. Schuste, F. Maury, Surf. Coat. Technol. 43 (1990) 185.
[22] K. Bewilogua, H.J. Heinitz, B. Rau, S. Schulze, Thin Solid Films 167 (1988) 233–243.
[23] M.T. Hernandez, M. González, A. De Pablos, Acta Mater. 51 (2003) 217–228.
[24] W.F. Chu, A. Rahmel, Oxid. Met. 15 (1981) 331–337.
[25] M.P. Antony, R. Vidhya, C.K. Mathews, U.V. Varada Raju, Thermochim. Acta 262 (1995) 145.
[26] E.K. Storms, The Refractory Carbides, New York, London, 1967, p. 102.
[27] M. Sternitzke, J. Eur. Ceram. Soc. 17 (1997) 1061–1082.
[28] S. Maensiri, S.G. Roberts, J. Eur. Ceram. Soc. 22 (2002) 2945–2956.
[29] M. Sternitzke, E. Dupas, P. Twigg, B. Derby, Acta Mater. 45 (10) (1997) 3963–3973.
[30] R.C. Bradt, J. Am. Ceram. Soc. 50 (1) (1967) 54–55.